International Journal of Geometric Methods in Modern Physics
(2026) 2650081 (21 pages)

DOI: 10.1142/S0219887826500817

On the kinematic-geometry of a line congruence

Areej A. Almoneef

Department of Mathematical Sciences, College of Science
Princess Nourah Bint Abdulrahman University
P. O. Box 84428, Riyadh 11671, Saudi Arabia
aaalmoneef@pnu.edu.sa

Rashad A. Abdel-Baky *

Department of Mathematics, Faculty of Science
University of Assiut, Assiut 71516, Egypt
rbaky@live.com

Received 15 May 2024
Accepted 18 October 2025
Published 21 November 2025

This study examines the kinematic geometry of line congruences in Euclidean 3-space $\mathbb{E}^3$, defined as two-parameter families of lines determined by a director surface and unit direction vectors. The fundamental properties of ruled surfaces within a line congruence are analyzed, with particular focus on their developability conditions and classification into torsal and non-torsal surfaces. The dual unit sphere representation is introduced, along with the fundamental forms of line congruences, leading to the derivation of mean and Gaussian curvature parameters. Additionally, the study explores the relationships between principal ruled surfaces and their curvature properties within the kinematic framework. Furthermore, Hamilton and Mannheim formulae are derived, offering deeper insights into the differential geometry and motion of line congruences.

Keywords: E. Study map; line congruence; distribution parameter.

Mathematics Subject Classification 2010: 53A04, 53A05, 53A17

1. Introduction

Differential line geometry explores families of lines in three-dimensional space, forming an organized framework known as a line space. This space can be Euclidean or non-Euclidean, depending on the underlying geometry. As a significant branch of differential geometry, it is closely related to spatial kinematics and plays a foundational role in various scientific and engineering fields. Its applications are particularly evident in robotic motion planning, where analyzing line trajectories enhances

*Corresponding author.

movement optimization and ensures seamless navigation. Additionally, in mechanical system design and kinematic analysis, line geometry facilitates the examination of motion chains, leading to more effective and precise mechanical systems [1–5]. Beyond robotics and mechanics, differential line geometry is widely utilized in computer graphics and vision, including shape reconstruction, stereo imaging, and motion tracking. Line-based models improve computational efficiency by reducing the complexity of three-dimensional representations. In optics, line congruences describe the propagation of light rays, making them essential for wavefront analysis, caustic formation, and the engineering of advanced optical instruments such as microscopes and telescopes. Furthermore, architectural engineering leverages ruled surfaces — a fundamental aspect of line geometry — to create innovative, lightweight structures that integrate both functionality and aesthetics.

A fundamental topic in this domain is the classification of differential line-geometric properties. A system of lines governed by two parameters is known as a line congruence, a structure that arises in numerous geometric and physical applications. A common example is the field of normal vectors of a surface, which forms a special type of line congruence. When a line congruence consists exclusively of normal lines to a surface, it is termed a normal line congruence [6, 7]. However, line congruences are not limited to surface normals; they also appear in fluid mechanics, where they represent streamlines and vortex filaments, contributing to the understanding of turbulent flows and aerodynamics. In structural engineering, they assist in designing adaptable frameworks and deployable structures that respond to external forces. Furthermore, in mathematical physics, line congruences provide insights into integrable systems and the differential equations governing motion and deformation. Given these extensive applications, the study of differential line geometry remains an active research field, with continuous advancements in both theoretical modeling and practical implementation across multiple disciplines. Research on line congruences has been extensive, with early work emphasizing their significance in geometric optics, particularly in studying light reflection and refraction. In differential geometry, a ruled surface — also referred to as a parametric ruled surface — arises when a family of straight lines (generators) in a congruence intersects a given curve on a surface. These surfaces are fundamental in kinematics, geometric design, and architectural engineering. Recent studies highlight the role of differential line geometry in understanding line congruences, emphasizing their importance in both theoretical and applied contexts [5–7].

A robust mathematical approach to analyzing motions in line space involves dual numbers, which provide an algebraic framework for spatial transformations. Through E. Study's mapping in screw theory and the algebra of dual numbers, the entirety of oriented lines in three-dimensional Euclidean space $\mathbb{E}^3$ can be systematically represented as points on the dual unit sphere in a three-dimensional dual space $\mathbb{D}^3$. This viewpoint has expanded research opportunities in ruled surface analysis and associated motions, particularly in dual spherical kinematics, where movements are governed by one or two parameters. These mathematical tools are crucial for

robotics, mechanical system design, and structural analysis, offering deeper insights into the geometric properties of line-based configurations. Further discussions on dual numbers, their relationship to ruled surfaces, and dual spherical motions can be found in [8–13]. Numerous applications exist for such investigations; for instance, consider [14, 15].

This research investigates line congruences in Euclidean 3-space $\mathbb{E}^3$, defined as two-parameter families of lines determined by a director surface and unit direction vectors. The study examines the fundamental properties of ruled surfaces within a line congruence, with particular emphasis on developability conditions and their classification into torsal and non-torsal surfaces. Using the dual unit sphere representation, the fundamental forms of line congruences are introduced, leading to the derivation of mean and Gaussian curvature parameters. The kinematic geometry of line congruences is also explored, establishing relationships between principal ruled surfaces and their curvature properties. Furthermore, Hamilton and Mannheim formulae are derived, providing deeper insights into the differential geometry and motion of line congruence. These findings contribute to the broader study of ruled surfaces, offering insights into their local and global geometric behavior.

2. Preliminaries

In this section, we use the same notation as in [6, 7]. For a more detailed discussion of the relevant properties, see [10–12]. The collection of dual numbers is given by

$$\mathbb{D} = \{\widehat{l} = l + \varepsilon l^* \,|\, l, \quad l^* \in, \varepsilon \neq 0, \varepsilon^2 = 0\}. \tag{1}$$

For any two dual numbers $\widehat{l} = l + \varepsilon l^*$and $\widehat{m} = m + \varepsilon m^*$ in $\mathbb{D}$, the following properties hold:

$$\left.\begin{aligned} &\widehat{l} = \widehat{m} = \Leftrightarrow l = m, \quad l^* = m^*, \\ &\widehat{l} + \widehat{m} = l + m + \varepsilon(l^* + m^*), \\ &\widehat{l}\widehat{m} = lm + \varepsilon(l^* m + m^* l). \end{aligned}\right\} \tag{2}$$

The division of dual numbers is given by

$$\frac{\widehat{l}}{\widehat{m}} = \frac{l}{m} + \varepsilon\left(\frac{l^* m - l m^*}{m^2}\right), \quad m \neq 0. \tag{3}$$

A dual number is classified as a pure dual number when it takes the form $\widehat{l} = \varepsilon l^*$, where division by such a number is not defined.

One application of dual numbers is in representing the dual angle between two skew lines in Euclidean space $\mathbb{E}^3$, which is given by

$$\widehat{\beta} = \beta + \varepsilon\beta^*, \tag{4}$$

where β represents the projected angle between the two lines, and β^* is the shortest distance between them along their common perpendicular. Based on these defini-

tions, we classify the relative positions of the lines as follows:

(1) If $\beta = \frac{\pi}{2}$ and $\beta^* = 0$, the lines intersect at a right angle.
(2) If $\beta = \frac{\pi}{2}$ and $\beta^* \neq 0$, the lines are orthogonal but skew.
(3) If $\beta \neq \frac{\pi}{2}$ and $\beta^* = 0$, the lines intersect.
(4) If $\beta = 0$ and $\beta^* = 0$, the lines are coincident, meaning they share the same orientation or are exactly opposite.

2.1. *E. Study mapping*

An oriented line can be described by a point $\mathbf{g} \in L$ and a unit direction vector $\mathbf{i}$ of L, satisfying $\|\mathbf{i}\|^2 = 1$. To establish a coordinate system for L, we define the moment vector as $\mathbf{i}^* = \mathbf{g} \times \mathbf{i}$, which is computed relative to the origin in Euclidean space $\mathbb{E}^3$. The vectors $\mathbf{i}$ and $\mathbf{i}^*$ are interconnected through the following relations:

$$\langle \mathbf{i}, \mathbf{i} \rangle = 1, \quad \langle \mathbf{i}^*, \mathbf{i} \rangle = 0. \tag{5}$$

The six coordinates $i_i,\ i_i^*(i = 1, 2, 3)$ of the vectors $\mathbf{i}$ and $\mathbf{i}^*$ are known as the Plücker coordinates of L. These vectors uniquely determine the oriented line L.

Conversely, any six-tuple $i_i,\ i_i^*(i = 1, 2, 3)$ satisfying the conditions

$$i_1^2 + i_2^2 + i_3^2 = 1, \quad i_1 i + i_2 i_2^* + i_3 i_3^* = 0 \tag{6}$$

defines a line in $\mathbb{E}^3$. Therefore, the collection of all oriented lines in $\mathbb{E}^3$ establishes a one-to-one correspondence with ordered pairs of vectors in $\mathbb{E}^3$, as described in Eq. (5).

For vectors $(\mathbf{i}^*, \mathbf{i}) \in \mathbb{E}^3 \times \mathbb{E}^3$ the set

$$\mathbb{D}^3 = \{\widehat{\mathbf{i}} = \mathbf{i} + \varepsilon \mathbf{i}^* \varepsilon \neq 0, \varepsilon 1 = 1\varepsilon, \varepsilon^2 = 0\} \tag{7}$$

defines the dual three-space $\mathbb{D}^3$, equipped with the scalar product

$$\langle \widehat{\mathbf{i}}, \widehat{\mathbf{i}} \rangle = \widehat{i}_1^2 + \widehat{i}_2^2 + \widehat{i}_3^2. \tag{8}$$

The norm of $\widehat{\mathbf{i}}$ is given by

$$\|\widehat{\mathbf{i}}\| = \|\mathbf{i}\| + \varepsilon \frac{\langle \mathbf{i}^*, \mathbf{i} \rangle}{\|\mathbf{i}\|}, \quad \|\mathbf{i}\| \neq 0. \tag{9}$$

A dual vector with a unit norm is referred to as a dual unit vector. From Eq. (7), it follows that a dual unit vector satisfies the conditions in Eq. (5). Consequently, any oriented line $L = (\mathbf{i}, \mathbf{i}^*) \in \mathbb{E}^3$ can be represented using a dual unit vector as

$$\widehat{\mathbf{i}} = \mathbf{i} + \varepsilon \mathbf{i}^* (\langle \mathbf{i}, \mathbf{i} \rangle + \varepsilon \langle \mathbf{i}^*, \mathbf{i} \rangle = 1). \tag{10}$$

The dual unit sphere in $\mathbb{D}^3$ is given by

$$\mathbb{K} = \{\widehat{\mathbf{i}} \in \mathbb{D}^3 \mid \|\widehat{\mathbf{i}}\|^2 = \widehat{i}_1^2 + \widehat{i}_2^2 + \widehat{i}_3^2 = 1\}. \tag{11}$$

According to the E. Study mapping, the set of points on the dual unit sphere in $\mathbb{D}^3$-space establishes a one-to-one correspondence with the set of all oriented lines in $\mathbb{E}^3$. This implies that the geometry of ruled surfaces in $\mathbb{E}^3$ is intrinsically linked to the geometry of curves on the dual unit sphere in $\mathbb{D}^3$. Therefore, in this framework, dual curves and ruled surfaces are considered equivalent [6, 7].

2.2. *Line congruence in Euclidean 3-space* $\mathbb{E}^3$

Using the notations introduced in the previous section, a line congruence is defined as a two-parameter family of lines in $\mathbb{E}^3$, expressed as

$$\mathbf{q}(v_1, v_2, \varsigma) = \mathbf{g}(v_1, v_2) + \varsigma \mathbf{e}(v_1, v_2),\ (v_1, v_2) \in \mathbb{D} \subseteq \mathbb{R} \times \mathbb{R}, \quad \varsigma \in \mathbb{R}, \tag{12}$$

where $\mathbf{g}(v_1, v_2)$ represents the director surface, and $\mathbf{e}(v_1, v_2)$ is the unit direction vector along the rulings, satisfying $\|\mathbf{e}\| = 1$. A ruled surface within the line congruence is parameterized by the equations:

$$v_1 = v_1(t), \quad v_2 = v_2(t), \quad v_1'^2 + v_2'^2 \neq 0, \quad t \in \mathbb{R} - \{0\}, \quad \left(' = \frac{d}{dt}\right) \tag{13}$$

This ruled surface is developable if and only if the condition $(\mathbf{e}, d\mathbf{g}, d\mathbf{e}) = 0$ is satisfied. Ruled surfaces, such as cones and cylinders, contain rulings where the tangent plane remains in contact with the surface along the entire line. Such rulings are called torsal lines, distinguishing them from non-torsal rulings in general cases [2, 3]:

- A ruled surface composed entirely of torsal rulings is called a developable surface.
- A ruled surface primarily consisting of non-torsal rulings is referred to as a non-developable ruled surface (or skew ruled surface).
- Cylinders, cones, and ruled surfaces generated by the tangents of a spatial curve are examples of developable surfaces.

Definition 2.1. A singular surface point along a torsal ruling is called a cuspidal point, and the tangent plane in any other direction at this point is known as the torsal plane.

Using the E. Study map, Eq. (11) can be expressed as

$$\widehat{\mathbf{e}}(v_1, v_2) = \mathbf{e}(v_1, v_2) + \varepsilon \mathbf{g}(v_1, v_2) \times \mathbf{e}(v_1, v_2). \tag{14}$$

Since $\|\mathbf{e}\| = 1$, it follows that $\widehat{\mathbf{e}}(v_1, v_2)$ also has unit magnitude, as shown by the following computation:

$$\|\widehat{\mathbf{e}}\| = \sqrt{\|\mathbf{e}\|^2 + 2\varepsilon\langle \mathbf{e}, \mathbf{g} \times \mathbf{e}\rangle + \varepsilon^2 \langle \mathbf{g} \times \mathbf{e}, \mathbf{g} \times \mathbf{e}\rangle} = \|\mathbf{e}\| = 1. \tag{15}$$

Thus, the line congruence occupies a region on the dual unit sphere in $\mathbb{D}^3$. Therefore, the line congruence can be described by

$$\widehat{\mathbf{e}}(v_1, v_2) = \mathbf{e}(v_1, v_2) + \varepsilon \mathbf{e}^*(v_1, v_2), \quad (v_1, v_2) \in \mathbb{D} \subseteq \mathbb{R} \times \mathbb{R}. \tag{16}$$

2.3. *Surfaces of the line congruence*

A relation of the form $f(v_1, v_2) = 0$, where v_1, v_2 are variables, defines a ruled surface within the line congruence. If these variables are parameterized as $v_i = v_i(t)$ for $i = 1, 2$, where $v_1(t)$ and $v_2(t)$ are functions of the real variable $t \in \mathbb{R}$, then $\widehat{\mathbf{e}}(v_1(t), v_2(t))$ represents a ruled surface in the line congruence. When v_2 is held

constant, say c_2, this condition describes either a ruled surface within the line congruence or a $\mathbb{D}$-curve on the dual unit sphere. The set of such curves traced by varying v_1-variable $\mathbb{D}$-curves. Likewise, fixing $v_1 = c_1$ results in a family of v_2-variable $\mathbb{D}$-curves on the dual unit sphere. Due to the established one-to-one correspondence between pairs of parameterized $\mathbb{D}$-curves and ruled surfaces in the line congruence, each $\mathbb{D}$-curve from one family intersects exactly one member from the other family.

Any two families of $\mathbb{D}$-curves fulfilling the last situations will supply us with parameter ruled surfaces which could appoint the line congruence. Hence, the line congruence can be distinguished as a 2-dimensional surface in $\mathbb{D}^3$. If $\mathcal{G}$ is any function (scalar or vector) defined for the line congruence, we denote its partial derivatives with respect to the parameters as $\mathcal{G}_{v_1}$, and $\mathcal{G}_{v_2}$ representing $\partial\mathcal{G}/\partial v_1$, and $\partial\mathcal{G}/\partial v_2$, respectively. Then, as shown in [6, 8]

$$\begin{aligned}\widehat{l} &= \langle \widehat{\mathbf{e}}_{v_1}, \widehat{\mathbf{e}}_{v_1} \rangle = l + \varepsilon l^*,\\ \widehat{m} &= \langle \widehat{\mathbf{e}}_{v_1}, \widehat{\mathbf{e}}_{v_2} \rangle = m + \varepsilon m^*,\\ \widehat{n} &= \langle \widehat{\mathbf{e}}_{v_2}, \widehat{\mathbf{e}}_{v_2} \rangle = n + \varepsilon n^*.\end{aligned} \tag{17}$$

The functions $\widehat{l}$, $\widehat{m}$, and $\widehat{n}$ are important because they allow us to determine the distance in the dual space between two neighboring points on the dual unit sphere. The magnitude of the differential displacement from dual unit sphere in $\mathbb{D}^3$ may be distinguished in view of them. The magnitude of the differential displacement from (v_1, v_2) to $(v_1 + dv_1, v_2 + dv_2)$ is given by

$$\begin{aligned}d\widehat{s}^2 &= \langle d\widehat{\mathbf{e}}, d\widehat{\mathbf{e}} \rangle = \langle \widehat{\mathbf{e}}_{v_1} dv_1 + \widehat{\mathbf{e}}_{v_2} dv_2, \widehat{\mathbf{e}}_{v_1} dv_1 + \widehat{\mathbf{e}}_{v_2} dv_2 \rangle\\ &= \widehat{l} dv_1^2 + 2\widehat{m} dv_1 dv_2 + \widehat{n} dv_2^2.\end{aligned} \tag{18}$$

From the real and dual parts, we obtain the following expressions for the 1st and 2nd fundamental forms of the line congruence

$$\mathcal{I} := ds^2 = l dv_1^2 + 2m dv_1 dv_2 + n dv_2^2 \tag{19}$$

and

$$\mathcal{II} := 2ds ds^* = l^* dv_1^2 + 2m^* dv_1 dv_2 + n^* dv_2^2. \tag{20}$$

Here $\mathcal{I}$ and $\mathcal{II}$ are are called the first and second principal forms of the line congruence, respectively. The first form $\mathcal{I}$ remains invariant under changes to the director surface, as this surface does not affect its calculation. Additionally, $\mathcal{I}$ is unaffected if we replace $\mathbf{e}$ by $-\mathbf{e}$. Thus, $\mathcal{I}$ represents a geometric invariant of the line congruence. In contrast, $\mathcal{II}$ is not an invariant of the line congruence itself but is instead an invariant of the pair $(\mathbf{e}, \mathbf{e}^*)$. Both $\mathcal{I}$ and $\mathcal{II}$ are invariant under Euclidean motions.

Let line congruence be a non-cylindrical line congruence ($ln - m^2 > 0$), then [6, 8]

$$\Delta = \frac{1}{2}\left(\frac{II}{I}\right) = \frac{l^* dv_1^2 + 2m^* dv_1 dv_{'2} + g^* dv_2^2}{l dv_1^2 + 2m dv_1 dv_{'2} + g dv_2^2} = \frac{l^* v_1^{'2} + 2m^* v_1^{'} u_{'2}^{'} + n^* v_2^{'2}}{l v_1^{'2} + 2m v_1^{'} v_{'2}^{'} + n v_2^{'2}} \tag{21}$$

is the distribution parameter of a ruled surface in line congruence. Δ is function of the ratio $v_1^{'}/v_2^{'}$, so it a function with the values of $v_1^{'}$ and $v_2^{'}$. This shows that the ruled surfaces which share the same Δ also share their central point and are therefore in 1st order contact. The extrema values of Δ are located by the minimum and maximum of the quotient in Eq. (20). There are two values for which Δ is a minimum or maximum. These are gained by equating to zero the derivatives of Δ via $v_1^{'}$ and $v_2^{'}$. This leads to the linear homogeneous system

$$\begin{pmatrix} 2\Delta l - l^* & 2\Delta m - m^* \\ 2\Delta m - m^* & 2\Delta n - n^* \end{pmatrix} \begin{pmatrix} v_1^{'} \\ v_2^{'} \end{pmatrix} = \begin{pmatrix} 0 \\ 0 \end{pmatrix}. \tag{22}$$

For a non-trivial solution $(v_1^{'}, v_2^{'}) \neq (0, 0)$ the left-hand side matrix must be singular, that is, Δ must fulfill the quadratic equation

$$(2\Delta l - l^*)(2\Delta n - n^*) - (2\Delta m - m^*)^2 = 0 \tag{23}$$

to be extrema. Because of $ln - m^2 > 0$, we gain

$$\Delta_{\max}, \Delta_{\min} = h \pm \sqrt{h^2 - k}, \tag{24}$$

where

$$\left.\begin{aligned} h(v_1, v_2) &= \frac{\Delta_{\max} + \Delta_{\min}}{2} = \frac{1}{4}\left(\frac{n^* l + l^* n - 2mm^*}{en - f^2}\right), \\ \kappa(v_1, v_2) &= \Delta_{\max}\Delta_{\min} = \frac{1}{4}\left(\frac{n^* l^* - m^{*2}}{ln - m^2}\right). \end{aligned}\right\} \tag{25}$$

Here h and κ are the mean and the Gaussian distribution parameters of the line congruence, respectively. It follows from Eq. (24) that

$$h^2 = k \Leftrightarrow \Delta_{\max} = \Delta_{\min}. \tag{26}$$

In this issue Δ is independent of any ratio $v_1^{'}/v_2^{'}$ and Eq. (21) must be vacuous, that is, they must be explained by any ratio $v_1^{'}/v_2^{'}$. This yields that each entry of the 2×2 matrix must vanish and the unique Δ is thus

$$\Delta = \frac{l^*}{2l} = \frac{m^*}{2m} = \frac{n^*}{2n}. \tag{27}$$

Thus the coefficients of $\mathcal{I}$ and $\mathcal{II}$ are commensurate, that is, the line congruence is an isotropic line congruence. Hence, we offer the next theorem [3, 6]:

Theorem 2.1. *In the Euclidean 3-space $\mathbb{E}^3$, through the lines of an isotropic line congruence, all ruled surfaces have 1st-order contact.*

2.4. *Principal and developable ruled surfaces*

We carry on with the extrema values of Δ. The ruled surfaces in the line congruence which have the extrema values of Δ are named principal ruled surfaces. The

principal ruled surfaces have the same role of principal lines (curvature lines) in surfaces theory. We may find them by eliminating Δ from Eq. (20), that [1,2]:

$$(l^*m - m^*l)v_1^{'2} + (l^*n - n^*l)v_1^{'}v_2^{'} + (m^*n - n^*m)v_2^{'2} = 0. \tag{28}$$

Under the hypotheses $m = m^* = 0$, we gain that $v_1^{'}v_2^{'} = 0$, so Eq. (27) shows that

$$(l^*m - m^*l) = 0, \quad (m^*n - n^*m) = 0.$$

Since the line congruence is non-isotropic, then

$$m = \langle \mathbf{e}_{v_1}, \mathbf{e}_{v_2} \rangle = 0, \quad m^* = \langle \mathbf{e}_{v_1}, \mathbf{e}^*_{v_2} \rangle + \langle \mathbf{e}^*_{v_1}, \mathbf{e}_{v_2} \rangle = 0 \Rightarrow \langle \widehat{\mathbf{e}}_{v_1}, \widehat{\mathbf{e}}_{v_2} \rangle = \widehat{m} = 0. \tag{29}$$

Therefore, their distribution parameters are

$$\Delta_{\max} = \frac{l^*}{2l}, \quad \Delta_{\min} = \frac{n^*}{2n}. \tag{30}$$

Then,

$$\left.\begin{aligned} h(v_1, v_2) &= \frac{\Delta_{\max} + \Delta_{\min}}{2} = \frac{1}{4}\left(\frac{l^*}{l} + \frac{n^*}{n}\right), \\ \kappa(v_1, v_2) &= \Delta_{\max}\Delta_{\min} = \frac{1}{4}\left(\frac{l^*n^*}{ln}\right). \end{aligned}\right\} \tag{31}$$

Proposition 1. *Consider a non-isotropic and non-cylindrical line congruence* $\widehat{\mathbf{e}}(v_1, v_2)$ *and let* $\widehat{\mathbf{e}}(t) = \widehat{\mathbf{e}}(v_1(t), v_2(t))$ *be a ruled surface within this line congruence. Then, the quantity* Δ *of* $\widehat{\mathbf{e}}(t)$ *attains an extremal value if and only if the ratio* $v_1^{'}/v_2^{'}$ *corresponds to a principal direction. Moreover, the principal ruled surfaces coincide with the parameter ruled surfaces.*

3. Kinematic-Geometry of a Line Congruence

In this section, we explore the concept of the kinematic geometry of a line congruence using fundamental formulas from surface theory. Moving forward, we assume $m = m^* = 0$. Under this particular condition, the dual arc-lengths are determined by first setting $dv_2 = 0$, followed by $dv_1 = 0$ in Eq. (17), yielding

$$d\widehat{s}_1 = ds_1 + \varepsilon ds_1^* = \widehat{p}_1 dv_1, \quad d\widehat{s}_2 = ds_2 + \varepsilon ds_2^* = \widehat{p}_2 dv_2, \tag{32}$$

where $\widehat{p}_1 = p_1 + \varepsilon p_1^* = \sqrt{\widehat{l}}$ and $\widehat{p}_2 = p_2 + \varepsilon p_2^* = \sqrt{\widehat{n}}$. The distribution parameters for the principal-ruled surfaces are then given by

$$\Delta_1 := \frac{ds_1^*}{ds_1} = \frac{l^*}{2l} \quad \text{and} \quad \Delta_2 := \frac{ds_2^*}{ds_2} = \frac{n^*}{2n}. \tag{33}$$

Furthermore, we define the following dual unit vectors:

$$\widehat{\mathbf{e}}_{12} = \frac{\widehat{\mathbf{e}}_{v_1}}{\sqrt{\widehat{l}}} = \frac{\widehat{\mathbf{e}}_{v_1}}{\sqrt{\langle \widehat{\mathbf{e}}_{v_1}, \widehat{\mathbf{e}}_{v_1} \rangle}}, \quad \widehat{\mathbf{e}}_{22} = \frac{\widehat{\mathbf{e}}_{v_2}}{\sqrt{\widehat{n}}} = \frac{\widehat{\mathbf{e}}_{v_2}}{\sqrt{\langle \widehat{\mathbf{e}}_{v_2}, \widehat{\mathbf{e}}_{v_2} \rangle}}, \quad \widehat{\mathbf{e}}_{12} \times \widehat{\mathbf{e}}_{22} = \widehat{\mathbf{e}}. \tag{34}$$

Thus, the set $\{\mathbf{0}, \widehat{\mathbf{e}}, \widehat{\mathbf{e}}_{12}, \widehat{\mathbf{e}}_{22}\}$ forms the Blaschke frame for the line congruence, satisfying the determinant condition $\det(\widehat{\mathbf{e}}, \widehat{\mathbf{e}}_{12}, \widehat{\mathbf{e}}_{22}) = +1$. Regarding the spherical

motions, the instantaneous movement of this frame corresponds to a rotation along the Darboux vector. For $\mathbb{D}$-curves given by $v_2 = c_2$ (which remain stationary in the real sense), the following relation holds:

$$\frac{\partial}{\partial \widehat{s}_1}\begin{pmatrix}\widehat{\mathbf{e}}\\ \widehat{\mathbf{e}}_{12}\\ \widehat{\mathbf{e}}_{22}\end{pmatrix} = \begin{pmatrix}0 & 1 & 0\\ -1 & 0 & \widehat{\chi}_1\\ 0 & -\widehat{\chi}_1 & 0\end{pmatrix}\begin{pmatrix}\widehat{\mathbf{e}}\\ \widehat{\mathbf{e}}_{12}\\ \widehat{\mathbf{e}}_{22}\end{pmatrix} = \widehat{\omega}_1 \times \begin{pmatrix}\widehat{\mathbf{e}}\\ \widehat{\mathbf{e}}_{12}\\ \widehat{\mathbf{e}}_{22}\end{pmatrix}, \tag{35}$$

where

$$\widehat{\omega}_1 = \widehat{\chi}_1\widehat{\mathbf{e}} + \widehat{\mathbf{e}}_{22} \quad \text{with } \widehat{\chi}_1 = \chi_1 + \varepsilon\chi_1^* = \frac{\widehat{l}_{v_2}}{2\widehat{l}\sqrt{\widehat{n}}}. \tag{36}$$

Similarly, for $\mathbb{D}$-curves where $v_1 = c_1$ (also real stationary), we have

$$\frac{\partial}{\partial \widehat{s}_2}\begin{pmatrix}\widehat{\mathbf{e}}\\ \widehat{\mathbf{e}}_{12}\\ \widehat{\mathbf{e}}_{22}\end{pmatrix} = \begin{pmatrix}0 & 0 & 1\\ 0 & 0 & \widehat{\chi}_2\\ -1 & -\widehat{\chi}_2 & 0\end{pmatrix}\begin{pmatrix}\widehat{\mathbf{e}}\\ \widehat{\mathbf{e}}_{12}\\ \widehat{\mathbf{e}}_{22}\end{pmatrix} = \widehat{\omega}_1 \times \begin{pmatrix}\widehat{\mathbf{e}}\\ \widehat{\mathbf{e}}_{12}\\ \widehat{\mathbf{e}}_{22}\end{pmatrix}, \tag{37}$$

where

$$\widehat{\omega}_2 = \widehat{\chi}_2\widehat{\mathbf{e}} - \widehat{\mathbf{e}}_{12}, \quad \text{with } \widehat{\chi}_2 = \chi_2 + \varepsilon\chi_2^* = \frac{\widehat{n}_{v_1}}{2\widehat{n}\sqrt{\widehat{l}}}. \tag{38}$$

Here, the quantities $\widehat{\chi}_i = \chi_i + \varepsilon\chi_i^*$ for $i = 1, 2$ represent the dual-geodesic curvatures of the principal-ruled surfaces. Additionally, they can be characterized as

$$\widehat{\chi}_i = \chi_i + \varepsilon\chi_i^* = \det\left(\widehat{\mathbf{e}}, \frac{d\widehat{\mathbf{e}}}{d\widehat{s}_i}, \frac{d^2\widehat{\mathbf{e}}}{d\widehat{s}_i^2}\right). \tag{39}$$

3.1. *Hamilton and Mannhiem formulae*

This subsection aims to establish the Hamilton and Mannheim formulae for the line congruence, analogous to their formulations in surface theory. Let $v_i = v_i(t)$ for $i = 1, 2$ be functions of the real variable t. Consequently, the function $\widehat{\mathbf{e}}(v_1(t), v_2(t))$ represents a parametrized ruled surface within the given line congruence. The tangent vector along this curve is given by

$$\widehat{\mathbf{e}}_t = \widehat{\mathbf{e}}_{v_1}\frac{dv_1}{dt} + \widehat{\mathbf{e}}_{v_2}\frac{dv_2}{dt}. \tag{40}$$

If $\|\widehat{\mathbf{e}}_t\| \neq 0$, we define

$$\widehat{\mathbf{e}}_2 = \frac{\widehat{\mathbf{e}}_t}{\|\widehat{\mathbf{e}}_t\|} = \frac{1}{\widehat{p}}\left(\widehat{\mathbf{e}}_{v_1}\frac{dv_1}{dt} + \widehat{\mathbf{e}}_{v_2}\frac{dv_2}{dt}\right), \tag{41}$$

where $\widehat{p} = p + \varepsilon p^* = \|\widehat{\mathbf{e}}_{v_1}\frac{dv_1}{dt} + \widehat{\mathbf{e}}_{v_2}\frac{dv_2}{dt}\| = \sqrt{\widehat{l}\widehat{n}}$. Thus, the dual arc length of the $\mathbb{D}$-curve $\widehat{\mathbf{e}}(v_1(t), v_2(t))$ is expressed as

$$d\widehat{s} = ds + \varepsilon ds^* = \widehat{p}dt. \tag{42}$$

The Blaschke frame associated with this $\mathbb{D}$-curve is

$$\left\{\widehat{\mathbf{e}}_1 = \widehat{\mathbf{e}}(t), \widehat{\mathbf{e}}_2 = \frac{\widehat{\mathbf{e}}_t}{\|\widehat{\mathbf{e}}_t\|}, \widehat{\mathbf{e}}_3(t) = \widehat{\mathbf{e}}_1 \times \widehat{\mathbf{e}}_2\right\}; \quad \det(\widehat{\mathbf{e}}_1, \widehat{\mathbf{e}}_2, \widehat{\mathbf{e}}_3) = +1. \tag{43}$$

The evolution of the frame along the arc length parameter $\widehat{s}$ is as follows:

$$\frac{\partial}{\partial \widehat{s}} \begin{pmatrix} \widehat{\mathbf{e}}_1 \\ \widehat{\mathbf{e}}_2 \\ \widehat{\mathbf{e}}_3 \end{pmatrix} = \begin{pmatrix} 0 & 1 & 0 \\ -1 & 0 & \chi \\ 0 & -\chi & 0 \end{pmatrix} \begin{pmatrix} \widehat{\mathbf{e}}_1 \\ \widehat{\mathbf{e}}_2 \\ \widehat{\mathbf{e}}_3 \end{pmatrix} = \omega \times \begin{pmatrix} \widehat{\mathbf{e}}_1 \\ \widehat{\mathbf{e}}_2 \\ \widehat{\mathbf{e}}_3 \end{pmatrix}, \tag{44}$$

where

$$\widehat{\omega} = \widehat{\chi}\widehat{\mathbf{e}}_1 + \widehat{\mathbf{e}}_3, \quad \text{with } \widehat{\chi} = \chi + \varepsilon\chi^* = \frac{\widehat{n}_{v_1}}{2\widehat{n}\sqrt{\widehat{l}}}. \tag{45}$$

Here $\widehat{\chi}$ is the $\mathbb{D}$-geodesic curvature of the parametrized ruled surface $\widehat{\mathbf{e}}(v_1(t), v_2(t))$. It follows that

$$\widehat{\chi} = \chi + \varepsilon\chi^* = \frac{\det(\widehat{\mathbf{e}}, \widehat{\mathbf{e}}_t, \widehat{\mathbf{e}}_{tt})}{\|\widehat{\mathbf{e}}_t\|^3} = \det\left(\widehat{\mathbf{e}}, \frac{d\widehat{\mathbf{e}}}{d\widehat{s}}, \frac{d^2\widehat{\mathbf{e}}}{d\widehat{s}^2}\right). \tag{46}$$

Since $\widehat{\mathbf{e}}_t$ is tangent to $\widehat{\mathbf{e}}(v_1(t), v_2(t))$, then using earlier relations, we obtain

$$\widehat{\mathbf{e}}_2 = \frac{d\widehat{s}_1}{d\widehat{s}}\widehat{\mathbf{e}}_{12} + \frac{d\widehat{s}_2}{d\widehat{s}}\widehat{\mathbf{e}}_{22}. \tag{47}$$

To further specify the motion, we introduce the dual angle $\widehat{\varphi} = \varphi + \varepsilon\varphi^*$, such that (Fig. 1)

$$\widehat{\mathbf{e}}_2 = \cos\widehat{\varphi}\widehat{\mathbf{e}}_{12} + \sin\widehat{\varphi}\widehat{\mathbf{e}}_{22}. \tag{48}$$

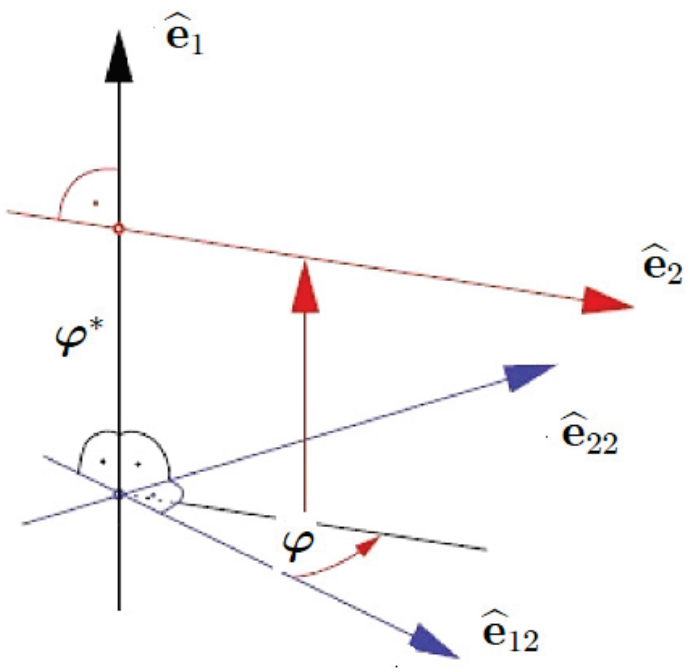

Fig. 1. $\widehat{\mathbf{e}}_2 = \cos\widehat{\varphi}\widehat{\mathbf{e}}_{12} + \sin\widehat{\varphi}\widehat{\mathbf{e}}_{22}$.

Here, the parameters satisfy

$$\left.\begin{aligned} &d\widehat{s}^2 = d\widehat{s}_1^2 + d\widehat{s}_2^2, \\ &\cos\widehat{\varphi} = \sqrt{\bar{l}}\frac{dv_1}{d\widehat{s}} = \frac{d\widehat{s}_1}{d\widehat{s}}, \quad \sin\widehat{\varphi} = \sqrt{\widehat{n}}\frac{dv_2}{d\widehat{s}} = \frac{d\widehat{s}_2}{d\widehat{s}}. \end{aligned}\right\} \tag{49}$$

By analyzing the real and dual components of these equations, along with prior results, we arrive at

$$\left.\begin{aligned} &\Delta = \Delta_1 \cos^2\varphi\Delta_1 + \Delta_2 \sin^2\varphi, \\ &\varphi^* = \frac{1}{2}(\Delta_2 - \Delta_1)\sin 2\varphi. \end{aligned}\right\} \tag{50}$$

These equations correspond to the Hamilton and Mannheim formulae in surface theory, respectively [6, 7].

3.2. *Plücker's conoid or cylindroid*

The surface characterized by φ^* in Eq. (50) exhibits symmetry with Plücker's conoid (or cylindroid) in surface theory. The cylindroid can also be represented using point coordinates: we assume that $\widehat{\mathbf{e}}_1$ is aligned with the positive x-axis of a stationary coordinate frame $(oxyz)$; while the dual unit vector $\widehat{\mathbf{e}}_2$is defined by the angle φ and the displacement φ^* along the x-axis. Thus, the dual unit vectors $\widehat{\mathbf{e}}_{12}$ and $\widehat{\mathbf{e}}_{22}$ serve as the principal axes, together with the directed $\widehat{\mathbf{e}}_1$ y and z -axes, respectively (as shown in Fig. 1). Hamilton's formula confirms that φ varies from 0 to $\frac{\pi}{2}$ as Δ transitions from Δ_1 to Δ_2, indicating that the principal ruled surfaces intersect at an angle of $\pi/2$. Thus the dual unit vectors $\widehat{\mathbf{e}}_{12}$ and $\widehat{\mathbf{e}}_{22}$ are the principal axes and jointly with the directed line $\widehat{\mathbf{e}}_1$, they form the fundamental coordinate framework of the cylindroid.

Let $\mathbf{r}$ be a point on this surface. Then, the parametrization of the cylindroid is given by

$$\mathcal{M} : \mathbf{r}(\varphi, \varphi^*, \varsigma) = (\varphi^*, 0, 0) + \varsigma(0, \cos\varphi, \sin\varphi), \quad \varsigma \in \mathbb{R}. \tag{51}$$

Clearly, the rulings of the surface pass through the x-axis, meaning

$$\mathcal{M} : \varphi^* := x = \frac{1}{2}(\Delta_2 - \Delta_1)\sin 2\varphi, \quad y = \varsigma\cos\varphi \quad \text{and} \quad z = \varsigma\sin\varphi. \tag{52}$$

Equation (52) establishes that the intersection of the principal axes $\widehat{\mathbf{e}}_{12}$ and $\widehat{\mathbf{e}}_{22}$ lies at half the height of the cylindroid φ^*. Consequently, we obtain the algebraic equation

$$\mathcal{M} : (y^2 + z^2)x + (\Delta_1 - \Delta_2)zy = 0. \tag{53}$$

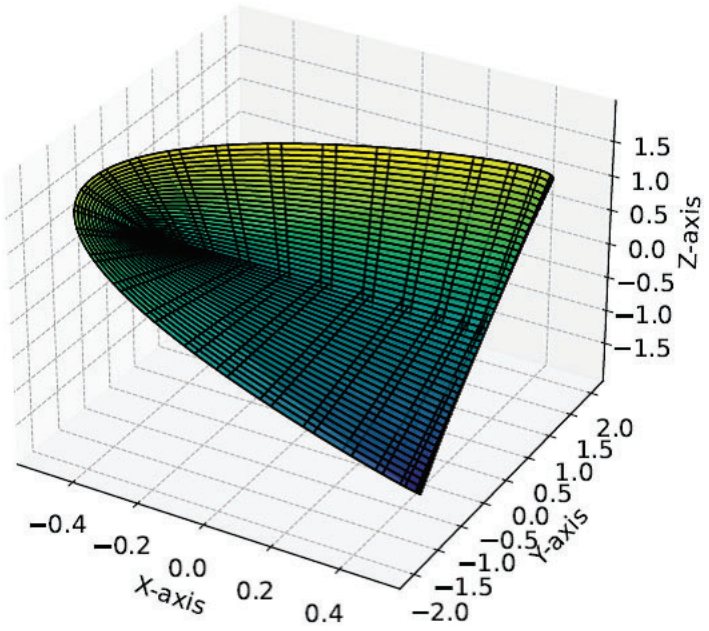

Fig. 2. The cylindroid.

The cylindroid has two integral invariants of the first order, which depend only on their difference: $\Delta_1 - \Delta_2 = 1,\ 0 \leq \varphi \leq 2\pi,\ -1 \leq \varsigma \leq 1$ (Fig. 2).

`Geometric properties of the cylindroid`

The cylindroid has two torsal planes π_1, π_2, each containing a torsal line L as described below.

(A) When $\Delta \neq 0$.

In this case, the parameter-ruled surface $\widehat{\mathbf{e}}(v_1(t), v_2(t))$ is non-developable surface. There exist two real rulings passing through the point $(x, 0, 0)$ only if $x < (\Delta_2 - \Delta_1)/2$. For the two limiting case $x = \pm(\Delta_2 - \Delta_1)/2$ the rulings coincide with the principal axes $\widehat{\mathbf{e}}_{12}$ and $\widehat{\mathbf{e}}_{22}$.

(B) When $\Delta = 0$.

In this case, the parameter-ruled surface $\widehat{\mathbf{e}}(v_1(t), v_2(t))$ is developable surface. The two torsal lines L_1, L_2 are given by

$$L_{1,2} : \frac{y}{z} = \tan\varphi = \pm\sqrt{-\frac{\Delta_1}{\Delta_2}}, \quad x = \pm(\Delta_2 - \Delta_1)/2. \tag{54}$$

These two torsal lines L_1, and L_2 intersect at a right angle. Furthermore, solving for y/z, we obtain a second-order algebraic equation whose roots are

$$\frac{y}{z} = \frac{1}{2x}[\Delta_2 - \Delta_1 \pm \sqrt{(\Delta_2 - \Delta_1)^2 - 4x^2}]. \tag{55}$$

Thus, the boundaries of the cylindroid, can be determined by setting the discriminant of Eq. (55) to zero, which gives the two extreme locations:

$$2x = \pm(\Delta_2 - \Delta_1). \tag{56}$$

Equation (56) defines the positions of the two torsal planes.

`Classification of the line congruence`

In this particular case, when the condition $\Delta_2 - \Delta_1 = 0$ holds, the cylindroid simplifies to a collection of lines passing through the origin within the torsal plane $x = 0$ (as well as the two torsal planes containing the x-axis). This type of line congruence is referred to as an elliptic line congruence. Conversely, if Δ_1 and Δ_2 have have opposite signs, the lines L_1 and L_2 remain real and align with the rulings $\widehat{\mathbf{e}}_{12}$ and $\widehat{\mathbf{e}}_{22}$, forming what is known as a hyperbolic line congruence. When either Δ_1 or Δ_2 equals zero, the resulting configuration is termed a parabolic line congruence, where both L_1 and L_2 coincide with the x-axis. Specifically, if $\Delta_1 \neq 0$ while $\Delta_2 = 0$ or vice versa, the lines instead align with the y-axis.

3.2.1. *J. Liouville's formula*

Once again, by differentiating Eq. (48) and utilizing the relation

$$\frac{d\widehat{\mathbf{e}}_2}{d\widehat{s}} = \frac{\partial\widehat{\mathbf{e}}_2}{\partial\widehat{s}_1}\frac{d\widehat{s}_1}{d\widehat{s}} + \frac{\partial\widehat{\mathbf{e}}_2}{\partial\widehat{s}_2}\frac{d\widehat{s}_2}{d\widehat{s}}, \tag{57}$$

we obtain

$$\frac{d\widehat{\mathbf{e}}_2}{d\widehat{s}} = \left(\frac{\partial\widehat{\mathbf{e}}_{12}}{\partial\widehat{s}_2} + \frac{\partial\widehat{\mathbf{e}}_{22}}{\partial\widehat{s}_1}\right)\sin\widehat{\varphi}\cos\widehat{\varphi} + \frac{\partial\widehat{\mathbf{e}}_{12}}{\partial\widehat{s}_1}\cos^2\widehat{\varphi} + \frac{\partial\widehat{\mathbf{e}}_{22}}{\partial\widehat{s}_2}\sin^2\widehat{\varphi}$$
$$+ (-\widehat{\mathbf{e}}_{12}\sin\widehat{\varphi} + \widehat{\mathbf{e}}_{22}\cos\widehat{\varphi})\frac{d\widehat{\varphi}}{d\widehat{s}}. \tag{58}$$

Furthermore, from Eqs. (43) and (48), we determine

$$\widehat{\mathbf{e}}_3 = -\sin\widehat{\varphi}\widehat{\mathbf{e}}_{12} + \cos\widehat{\varphi}\widehat{\mathbf{e}}_{22}. \tag{59}$$

Applying Eqs. (35), (37), and (47), Eq. (58) simplifies to

$$\frac{d\widehat{\mathbf{e}}_2}{d\widehat{s}} := \widehat{\mathbf{e}}_1 + \widehat{\chi}\widehat{\mathbf{e}}_3 = \left(\widehat{\chi}_1\cos\widehat{\varphi} + \widehat{\chi}_2\sin\widehat{\varphi} - \frac{d\widehat{\varphi}}{d\widehat{s}}\right)\widehat{\mathbf{e}}_3 + \widehat{\mathbf{e}}_1.$$

Thus, we establish

$$\widehat{\chi} = \widehat{\chi}_1\cos\widehat{\varphi} + \widehat{\chi}_2\sin\widehat{\varphi} - \frac{d\widehat{\varphi}}{d\widehat{s}}, \tag{60}$$

which corresponds to J. Liouville's formula in surface theory [1–4, 7].

Theorem 3.1. *For the line congruence $\widehat{\mathbf{e}}(v_1, v_2)$ there exists a relation involving the Darboux vectors of the Blaschke frames given by*

$$\widehat{\omega} = \cos\widehat{\varphi}\widehat{\omega}_1 + \sin\widehat{\varphi}\widehat{\omega}_2 - \left(\frac{d\widehat{\varphi}}{d\widehat{s}}\right)\widehat{\mathbf{e}}_1. \tag{61}$$

Proof. By substituting Eq. (59) into Eq. (45), we express $\widehat{\omega}$ as

$$\widehat{\omega} = \widehat{\chi}\widehat{\mathbf{e}}_1 - \sin\widehat{\varphi}\widehat{\mathbf{e}}_{12} + \cos\widehat{\varphi}\widehat{\mathbf{e}}_{22}.$$

Using Eqs. (36) and (38), this can be rewritten as

$$\widehat{\omega} = (\widehat{\chi} - \widehat{\chi}_1\cos\widehat{\varphi} - \widehat{\chi}_2\sin\widehat{\varphi})\widehat{\mathbf{e}}_1 + \cos\widehat{\varphi}\widehat{\omega}_1 + \sin\widehat{\varphi}\widehat{\omega}_2. \tag{62}$$

Finally, incorporating the geodesic curvature from Eq. (60) into Eq. (62), we retrieve Eq. (61). □

3.3. *The dual angle of pitch*

It is well known that the dual angle of pitch serves as a fundamental invariant for a closed ruled surface, as demonstrated in various studies [13, 16–18]. Consequently, we introduce an alternative geometric interpretation. To begin, we establish the following relations:

$$\left.\begin{aligned}
\frac{\partial\widehat{\mathbf{e}}_2}{\partial\widehat{s}_1} &= -\cos\widehat{\varphi}\widehat{\mathbf{e}}_1 + \left(\frac{\partial\widehat{\varphi}}{\partial\widehat{s}_1} + \widehat{\varkappa}_1\right)\widehat{\mathbf{e}}_3,\\
\frac{\partial\widehat{\mathbf{e}}_2}{\partial\widehat{s}_2} &= -\sin\widehat{\varphi}\widehat{\mathbf{e}}_1 + \left(\frac{\partial\widehat{\varphi}}{\partial\widehat{s}_2} + \widehat{\varkappa}_2\right)\widehat{\mathbf{e}}_3,\\
\frac{\partial\widehat{\mathbf{e}}_3}{\partial\widehat{s}_1} &= \sin\widehat{\varphi}\widehat{\mathbf{e}}_1 - \left(\frac{\partial\widehat{\varphi}}{\partial\widehat{s}_1} + \widehat{\varkappa}_1\right)\widehat{\mathbf{e}}_2,\\
\frac{\partial\widehat{\mathbf{e}}_3}{\partial\widehat{s}_2} &= -\cos\widehat{\varphi}\widehat{\mathbf{e}}_1 - \left(\frac{\partial\widehat{\varphi}}{\partial\widehat{s}_2} + \widehat{\varkappa}_2\right)\widehat{\mathbf{e}}_2.
\end{aligned}\right\} \tag{63}$$

Next, for a parameterized ruled surface satisfying

$$\widehat{\mathbf{e}}_1(v_1(t), v_2(t)) = \widehat{\mathbf{e}}_1(v_1(t+2\pi), v_2(t+2\pi)), \quad t \in \mathbb{R}, \tag{64}$$

we can characterize the closure condition. Additionally, in the plane $Sp\{\widehat{\mathbf{e}}_2, \widehat{\mathbf{e}}_3\}$, we define the dual unit vector as

$$\widehat{\mathbf{n}} = \cos\widehat{\beta}\widehat{\mathbf{e}}_2 + \sin\widehat{\beta}\widehat{\mathbf{e}}_3 \quad \text{with } \beta + \varepsilon\beta^*, \tag{65}$$

which describes a developable ruled surface (torse) passing through the orthogonal trajectory of the $\widehat{\mathbf{e}}_1(t)$-closed ruled surface. If we denote the dual angle of pitch of the $\widehat{\mathbf{e}}_1(t)$-closed ruled surface by Σ, then it is given by

$$\Sigma := \lambda - \varepsilon\Gamma = \oint d\widehat{\beta}, \tag{66}$$

where λ represents the pitch angle and Γ denotes the pitch of the closed ruled surface $\widehat{\mathbf{e}}_1(t)$-closed ruled surface. In fact, from Eqs. (65) and (66), we find that

$$\Sigma := -\oint\langle d\widehat{\mathbf{e}}_2, \widehat{\mathbf{e}}_3\rangle = \oint\langle d\widehat{\mathbf{e}}_3, \widehat{\mathbf{e}}_2\rangle. \tag{67}$$

From this, it follows that

$$-\Sigma = \oint \left\langle \frac{\partial \widehat{\mathbf{e}}_2}{\partial \widehat{s}_1} d\widehat{s}_1 + \frac{\partial \widehat{\mathbf{e}}_2}{\partial \widehat{s}_2} d\widehat{s}_2, \widehat{\mathbf{e}}_3 \right\rangle$$
$$= \oint \left[\left\langle \frac{\partial \widehat{\mathbf{e}}_2}{\partial \widehat{s}_1}, \widehat{\mathbf{e}}_3 \right\rangle d\widehat{s}_1 + \left\langle \frac{\partial \widehat{\mathbf{e}}_2}{\partial \widehat{s}_2}, \widehat{\mathbf{e}}_3 \right\rangle d\widehat{s}_2 \right] \tag{68}$$

Applying Green's theorem, we obtain

$$-\Sigma = \iint \left[\frac{\partial}{\partial \widehat{s}_1} \left(\left\langle \frac{\partial \widehat{\mathbf{e}}_2}{\partial \widehat{s}_2}, \widehat{\mathbf{e}}_3 \right\rangle \right) - \frac{\partial}{\partial \widehat{s}_2} \left(\left\langle \frac{\partial \widehat{\mathbf{e}}_2}{\partial \widehat{s}_1}, \widehat{\mathbf{e}}_3 \right\rangle \right) \right] d\widehat{s}_1 d\widehat{s}_2. \tag{69}$$

Using Eq. (61) and the symmetry property $\frac{\partial}{\partial \widehat{s}_1}(\frac{\partial \widehat{\mathbf{e}}_2}{\partial \widehat{s}_2}) = \frac{\partial}{\partial \widehat{s}_2}(\frac{\partial \widehat{\mathbf{e}}_2}{\partial \widehat{s}_1})$, we conclude that

$$-\Sigma := \iint d\widehat{s}_1 d\widehat{s}_2 = \iint d\widehat{a}, \tag{70}$$

where $d\widehat{a} := da + \varepsilon da^* = d\widehat{s}_1 d\widehat{s}_2$ represents the $\mathbb{D}$-area on the dual unit sphere bounded by the closed trajectory $\widehat{\mathbf{e}}_1(t) = \widehat{\mathbf{e}}_1(t + 2\pi)$.

Theorem 3.2. *In $\mathbb{E}^3$, the dual angle of pitch of a closed ruled surface corresponds to the negative total dual spherical area of its dual image.*

However, using Eqs. (32) and (67), we obtain

$$-\Sigma = \iint (1 + \varepsilon\Delta_1)(1 + \varepsilon\Delta_2) ds_1 ds_2$$
$$= \iint ds_1 ds_2 + \varepsilon \iint (\Delta_1 + \Delta_2) ds_1 ds_2.$$

Thus, by distinguishing between the real and dual components, we establish the following relationships:

$$\lambda = -a \quad \text{and} \quad \Gamma = \iint (\Delta_1 + \Delta_2) ds_1 ds_2.$$

Here, $a = \iint ds_1 ds_2$ represents the spherical area on the real unit sphere enclosed by the closed trajectory $\mathbf{e}_1(t) = \mathbf{e}_1(t + 2\pi)$.

3.4. *Examples and remarks*

In this subsection, we present illustrative models to verify the approach.

Example 1. The dual coordinates $\widehat{e}_i = (e_i + \varepsilon e_i^*)$ for an arbitrary point $\widehat{\mathbf{e}} \in \mathbb{K}$, centered at the origin, can be expressed as

$$\widehat{\mathbf{e}}(\widehat{\varkappa}, \widehat{\varsigma}) :== (\cos\widehat{\varkappa}\sin\widehat{\varsigma}, \sin\widehat{\varkappa}\sin\widehat{\varsigma}, \cos\widehat{\varsigma}), \tag{71}$$

where $\widehat{\varkappa} = \varkappa + \varepsilon\varkappa^*$ and $\widehat{\varsigma} = \varsigma + \varepsilon\varsigma^*$ are $\mathbb{D}$-angles with $\varkappa^*$, $\varsigma^* \in \mathbb{R}$, $0 \le \varkappa \le 2\pi$ and $0 \le \varsigma \le \pi/2$, respectively. By separating real and dual components, we obtain

$$\left.\begin{aligned} e_1 &= \cos\varkappa\sin\varsigma, \quad e_1^* = -\varkappa^*\sin\varkappa\sin\varsigma + \varsigma^*\cos\varkappa\cos\varsigma, \\ e_2 &= \sin\varkappa\sin\varsigma, \quad e_2^* = \varkappa^*\cos\varkappa\sin\varsigma + \varsigma^*\sin\varkappa\cos\varsigma, \\ e_3 &= \cos\varsigma, \quad e_3^* = -\varsigma^*\sin\varsigma. \end{aligned}\right\} \tag{72}$$

The equations above describe a four-parameter motion of a line in $\mathbb{E}^3$. To obtain a line congruence in $\mathbb{E}^3$, we define $\widehat{\varkappa} = (\varkappa, \varsigma)$ and $\widehat{\varsigma} = (\varkappa, \varsigma)$, leading to the line congruence

$$\begin{aligned}\widehat{\mathbf{e}}(\varkappa,\varsigma) = (\cos\varkappa\sin\varsigma, \sin\varkappa\sin\varsigma, \cos\varsigma) + \varepsilon[\varkappa^*(-\sin\varkappa\sin\varsigma, \cos\varkappa\sin\varsigma, 0)\\ + \varsigma^*(\cos\varkappa\cos\varsigma, \sin\varkappa\cos\varsigma, -\sin\varsigma)].\end{aligned} \tag{73}$$

Using Eqs. (72) and (16), we derive

$$\begin{aligned} l &= \sin^2\varsigma, \quad m = 0, \quad n = 1,\\ l^* &= 2\left(\frac{\partial\varkappa^*}{\partial\varkappa}\sin\varsigma + \varsigma^*\cos\varsigma\right)\sin\varsigma,\\ m^* &= \left(\frac{\partial\varkappa^*}{\partial\varsigma}\sin^2\varsigma + \frac{\partial\varsigma^*}{\partial\varkappa}\right), \quad n^* = 2\frac{\partial\varsigma^*}{\partial\varsigma}.\end{aligned} \tag{74}$$

Thus, we obtain

$$\Delta(\varkappa,\varsigma) = \frac{(\frac{\partial\varkappa^*}{\partial\varkappa}\sin\varsigma + \varsigma^*\cos\varsigma)\sin\varsigma d\varkappa^2 + (\frac{\partial\varkappa^*}{\partial\varsigma}\sin^2\varsigma + \frac{\partial\varsigma^*}{\partial\varkappa})d\varkappa d\varsigma + \frac{\partial\varsigma^*}{\partial\varsigma}d\varsigma^2}{\sin^2\varsigma d\varkappa^2 + d\varsigma^2}. \tag{75}$$

`Principal ruled surfaces of the line congruence`

Let $\zeta = \frac{d\varkappa}{d\varsigma}$. Using Eqs. (27) and (74), we obtain the quadratic equation

$$\begin{aligned}\sin^2\varsigma\left(\frac{\partial\varkappa^*}{\partial\varsigma}\sin\varsigma + \frac{\partial\varsigma^*}{\partial\varkappa}\right)\zeta^2 + 2\sin^2\varsigma\left(\frac{\partial\varkappa^*}{\partial\varkappa}\sin\varsigma + \varsigma^*\cos\varsigma\right)\zeta\\ + \left(\frac{\partial\varkappa^*}{\partial\varsigma}\sin^2\varsigma + \frac{\partial\varsigma^*}{\partial\varkappa}\right) = 0.\end{aligned} \tag{76}$$

Since this equation is quadratic in ζ setting its coefficients to zero yields

$$\begin{aligned}\frac{\partial\varkappa^*}{\partial\varsigma}\sin^2\varsigma + \frac{\partial\varsigma^*}{\partial\varkappa} = 0,\\ \frac{\partial\varkappa^*}{\partial\varkappa}\sin\varsigma + \varsigma^*\cos\varsigma = 0,\\ \frac{\partial\varkappa^*}{\partial\varsigma}\sin^2\varsigma + \frac{\partial\varsigma^*}{\partial\varkappa} = 0.\end{aligned} \tag{77}$$

These partial differential equations determine the principal ruled surfaces of the line congruence. Given that $\varsigma^* = -\varkappa + \varsigma$ and $\varkappa^* = \varkappa + \varsigma$, we obtain

$$\sin^2 \varsigma - 1 = 0, \quad 1 + (-\varkappa + \varsigma)\cot \varsigma = 0 \Rightarrow \varsigma = \pm\frac{\pi}{2}. \tag{78}$$

By substituting these results into Eq. (73), we derive

$$\begin{aligned}\widehat{\mathbf{e}}(\varkappa) &= \pm(\cos \varkappa, \sin \varkappa, 0) \\ &\quad + \varepsilon\left[\left(\varkappa \pm \frac{\pi}{2}\right)(\mp \sin \varkappa, \pm \cos \varkappa, 0) + \left(-\varkappa \pm \frac{\pi}{2}\right)(0, 0, \mp 1)\right].\end{aligned} \tag{79}$$

Thus, we obtain

$$h(\varkappa, v) = \pm\frac{1}{4}(\pm 1 + 2), \quad \kappa(\varkappa, v) = \pm\frac{1}{2}. \tag{80}$$

Thus, the principal ruled surfaces of the line congruence are

$$\begin{aligned}\mathbf{P}_1(\varkappa, v) = \Big(&\left(-\varkappa + \frac{\pi}{2}\right)\sin \varkappa + v \cos \varkappa, -\left(-\varkappa + \frac{\pi}{2}\right)\cos \varkappa \\ &+ v \sin \varkappa, \varkappa + \frac{\pi}{2}\Big), \quad v \in \mathbb{R}\end{aligned} \tag{81}$$

and

$$\begin{aligned}\mathbf{P}_2(\varkappa, v) = \Big(&-\left(\varkappa + \frac{\pi}{2}\right)\sin \varkappa - v \cos \varkappa, \left(\varkappa + \frac{\pi}{2}\right)\cos \varkappa \\ &- v \sin \varkappa, \varkappa - \frac{\pi}{2}\Big), \quad v \in \mathbb{R}.\end{aligned} \tag{82}$$

For $-2 \leq v \leq -2$, and $0 \leq \varkappa \leq 2\pi$ the corresponding principal ruled surfaces are depicted in Fig. 3.

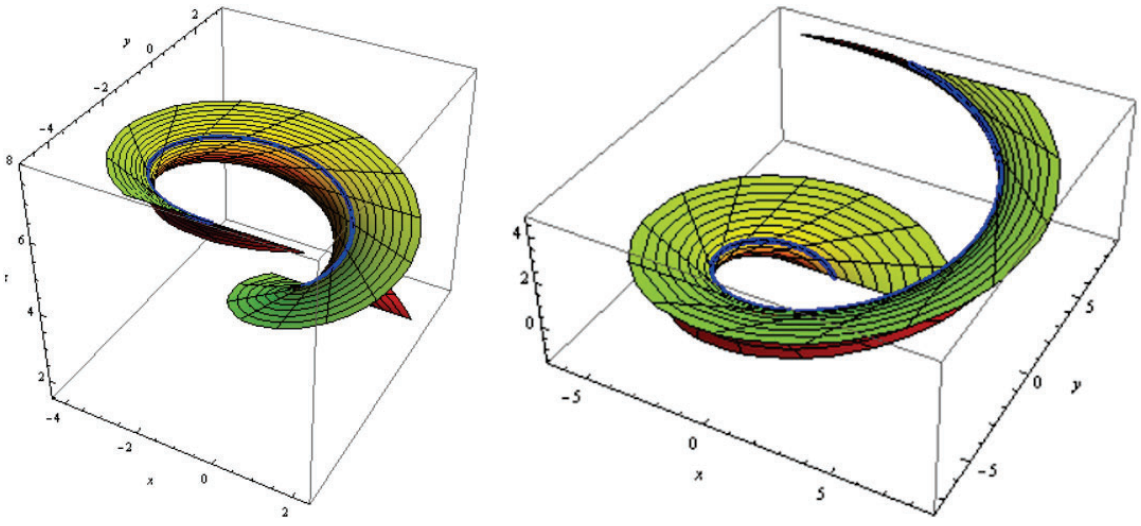

Fig. 3. The principal ruled surfaces.

Developable ruled surfaces of the line congruence

Let $\Delta(\varkappa,\varsigma)=0$, and $\zeta=\frac{d\varkappa}{d\varsigma}$. Then,

$$\left(\frac{\partial\varkappa^*}{\partial\varkappa}\sin\varsigma+\varsigma^*\cos\varsigma\right)\sin\varsigma\zeta^2+\left(\frac{\partial\varkappa^*}{\partial\varsigma}\sin^2\varsigma+\frac{\partial\varsigma^*}{\partial\varkappa}\right)\zeta+\frac{\partial\varsigma^*}{\partial\varsigma}=0, \tag{83}$$

which leads to the conditions:

$$\frac{\partial\varkappa^*}{\partial\varkappa}\sin\varsigma+\varsigma^*\cos\varsigma=0,\quad \frac{\partial\varkappa^*}{\partial\varsigma}\sin^2\varsigma+\frac{\partial\varsigma^*}{\partial\varkappa}=0,\quad \frac{\partial\varsigma^*}{\partial\varsigma}=0. \tag{84}$$

Solving the above partial differential equations yields

$$\varkappa^*=\pm(\cos\varkappa-\sin\varkappa)\cot\varsigma,\quad \varsigma^*=\pm(\cos\varkappa+\sin\varkappa).$$

Thus, the developable ruled surfaces can be characterized as follows: Since $\mathbf{g}\times\mathbf{e}=\mathbf{e}^*$, it follows that

$$\left.\begin{aligned} g_2\cos\varsigma-g_3\sin\varkappa\sin\varsigma&=e_1^*,\\ -g_1\cos\varsigma+g_3\cos\varkappa\sin\varsigma&=e_2^*,\\ (g_1\sin\varkappa-g_2\cos\varkappa)\sin\varsigma&=e_3^*.\end{aligned}\right\}$$

The coefficient matrix for the unknowns g_1, g_2, and g_3 is

$$\begin{pmatrix} 0 & \cos\varsigma & -\sin\varkappa\sin\varsigma\\ -\cos\varsigma & 0 & \cos\varkappa\sin\varsigma\\ \cos\varkappa\sin\varsigma & -\cos\varkappa\sin\varsigma & 0\end{pmatrix},$$

which has rank 2. The rank of the augmented matrix

$$\begin{pmatrix} 0 & \cos\varsigma & -\sin\varkappa\sin\varsigma & e_1^*\\ -\cos\varsigma & 0 & \cos\varkappa\sin\varsigma & e_2^*\\ \sin\varkappa\sin\varsigma & -\cos\varkappa\sin\varsigma & 0 & e_3^*\end{pmatrix}$$

is also 2; where $0\le\varkappa\le2\pi$ and $0\le\varsigma\le\pi/2$. Hence, this system has infinitely many solutions, given by

$$\begin{aligned} g_1\sin\varkappa-g_2\cos\varkappa&=-\varsigma^*,\\ g_1&=(g_3-\varkappa^*)\tan\varsigma\cos\varkappa-\varsigma^*\sin\varkappa,\\ g_2&=(g_3-\varkappa^*)\tan\varsigma\cos\varkappa+\varsigma^*\cos\varkappa.\end{aligned} \tag{85}$$

Since g_3 is arbitrary, we set $g_3=\varkappa^*$, leading to the director surface:

$$\mathbf{g}(\varkappa,\varsigma)=(\pm(\cos\varkappa+\sin\varkappa)\sin\varkappa,\pm(\cos\varkappa+\sin\varkappa)\cos\varkappa,\pm(\cos\varkappa-\sin\varkappa)\cot\varsigma).$$

Consequently, the line congruence takes the form

$$\mathbf{q}(\varkappa,\varsigma,v)=\begin{pmatrix}\pm(\cos\varkappa+\sin\varkappa)\sin\varkappa+v\cos\varkappa\sin\varsigma\\ \pm(\cos\varkappa+\sin\varkappa)\cos\varkappa+v\sin\varkappa\sin\varsigma\\ \pm(\cos\varkappa-\sin\varkappa)\cot\varsigma+v\cos\varsigma\end{pmatrix},\quad v\in\mathbb{R}. \tag{86}$$

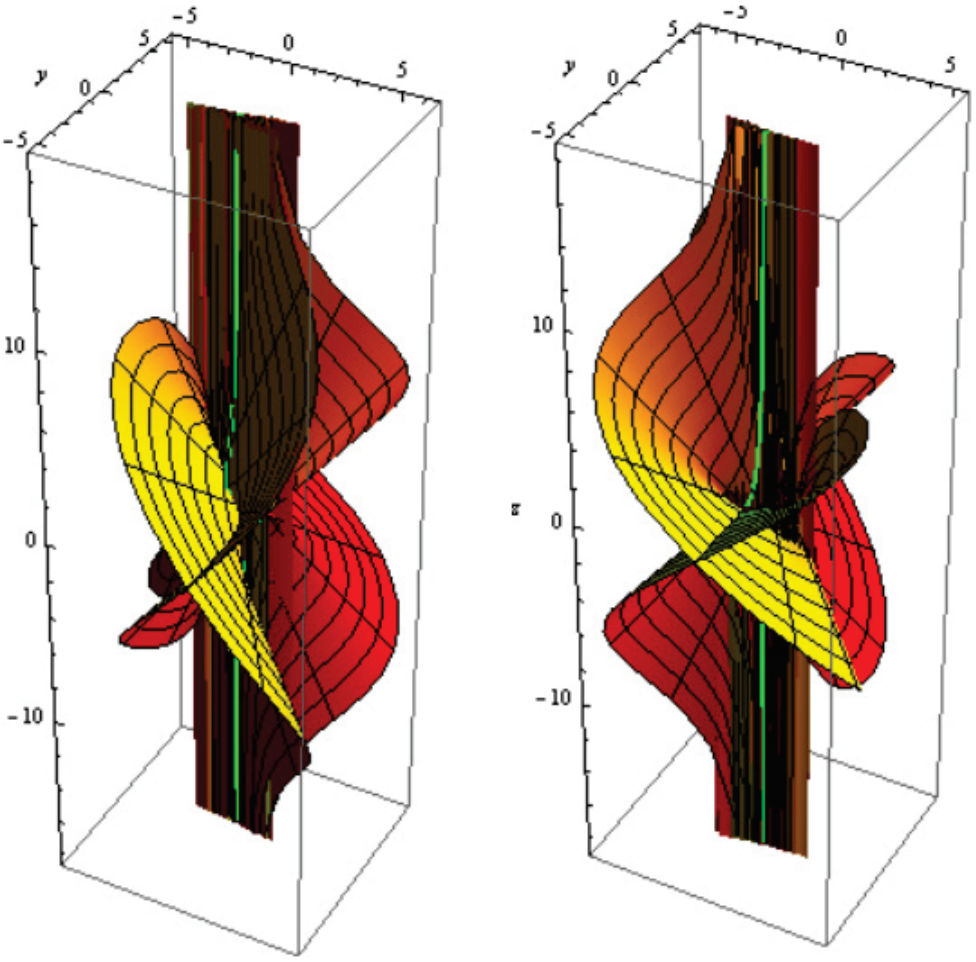

Fig. 4. The developable ruled surfaces.

It is clear that once $\varkappa$, and ς are specified, the developable ruled surfaces can be determined. When setting $\varsigma(u) = \varkappa(u) = u$, with $-11 \leq v \leq -11$, and $0 \leq u \leq 2\pi$ the developable ruled surfaces are visualized in Fig. 4.

4. Conclusion

In this study, we have examined the fundamental geometric properties of a line congruence in $\mathbb{E}^3$, including its parameterization, principal ruled surfaces, and associated curvature measures. By utilizing the E. Study map and dual unit sphere representations, we established a rigorous framework for analyzing both developable and non-developable ruled surfaces within a given line congruence. The distribution parameters and their extrema play a crucial role in classifying the principal ruled surfaces, while the introduction of kinematic geometry concepts further enhances our understanding of line congruences in the context of Euclidean differential geometry.

Future research may explore the role of Lie group structures in governing transformations of line congruences, as well as extend these results to broader geometric

settings such as affine and projective spaces. Additionally, we aim to integrate insights from submanifold theory and singularity theory, as discussed in [19, 20], to further investigate the implications of our findings. This approach may lead to new theorems concerning symmetric properties in this domain.

Acknowledgments

The authors express their sincere thanks to the anonymous reviewers for their careful reading of their paper and their insightful comments and suggestions. The authors also would like to acknowledge the Princess Nourah bint Abdulrahman University Researchers Supporting Project number (PNURSP2025R337), Princess Nourah bint Abdulrahman University, Riyadh, Saudi Arabia.

ORCID

Areej A. Almoneef https://orcid.org/0000-0001-7041-3730

Rashad A. Abdel-baky https://orcid.org/0000-0001-7016-9280

References

[1] O. Bottema and B. Roth, *Theoretical Kinematics* (North-Holland Press, New York, 1979).
[2] A. Karger and J. Novak, *Space Kinematics and Lie Groups* (Gordon and Breach Science Publishers, New York, 1985).
[3] H. Pottman and J. Wallner, *Computational Line Geometry* (Springer-Verlag, Berlin, Heidelberg, 2001).
[4] B. Odehnal and H. Pottmann, Computing with discrete models of ruled surfaces and line congruences, in *Proc. 2nd Workshop on Computational Kinematics* (Seoul, 2001).
[5] O. Odehnal, Geometric optimization methods for line congruences, thesis, Vienna University of Technology (2002).
[6] W. Blaschke, *Vorlesungen über Differential Geometrie*, *Band* 1 (Dover Publications, New York, 1945), pp. 260–277.
[7] L. P. Eisenhart, *A Treatise in Differential Geometry of Curves and Surfaces* (Ginn & company, New York, 1969).
[8] R. A. Abdel-Baky, On a line congruence which has the parameter ruled surfaces as principal ruled surfaces, *Appl. Math. Comput.* **151**(3) (2004) 849–862.
[9] R. A. Abdel-Baky and F. R. Al-Solamy, A new geometrical approach to one-parameter spatial motion, *J. Eng. Math.* **60** (2008) 149–172.
[10] F. Tas and O. Gürsoy, On the line congruences, *Int. Electron. J. Geom.* **11** (2018) 1–7.
[11] R. A. Abdel-Baky and M. F. Naghi, A study on a line congruence as surface in the space of lines, *AIMS Math.* **6**(10) (2021) 11109–11123.
[12] Y. Li, F. Mofarreh and R. A. Abdel-Baky, Kinematic-geometry of a line trajectory and the invariants of the axodes, *Demonstr. Math.* **56** (2023) 20220252.
[13] A. A. Almoneef and R. A. Abdel-Baky, Timelike constant axis ruled surface family in Minkowski 3-space, *Symmetry* **16** (2024) 677, doi:10.3390/sym16060677.

[14] A. Hegazy, M. Abdel-Megied, A. Gedamy and M. Abdelgaber, Bulk viscous plane-symmetric cosmological model in Lyra's geometry and general relativity theory, *Int. J. Geom. Methods Mod. Phys.* **10**(1) (2023) 5–10.
[15] F. N. M. Al-Showaikh, The exact endoscopic effect and non-uniform geometry on the peristaltic flow, *Appl. Math. Inf. Sci.* **18**(5) (2024) 1029–1035, doi:10.18576/amis/180510.
[16] O. Gorsoy, The dual angle of pitch of a closed ruled surface, *Mech. Mach. Theory* **25** (1990) 131–140.
[17] M. T. Aldossary and R. A. Abdel-Baky, On the Bertrand offsets for ruled and developable surfaces, *Boll. Unione Mat. Ital.* **8** (2015) 53–64.
[18] R. A. Abdel-Baky and F. Mofarreh, A study on the Bertrand offsets of timelike ruled surfaces in Minkowski 3-space, *Symmetry* **14**(4) (2022) 783.
[19] Y. L. Li, Y. S. Zhu and Q. Y. Sun, Singularities and dualities of pedal curves in pseudo-hyperbolic and de Sitter space, *Int. J. Geom. Methods Mod. Phys.* **18** (2021) 1–31.
[20] Y. L. Li, S. Nazra and R. A. Abdel-Baky, Singularities properties of timelike sweeping surface in Minkowski 3-space, *Symmetry* **14** (2022) 1996, doi:10.3390/sym14101996.